LTU Journal of Advanced Computing & Engineering (LTU-JACE)

ISSN: 3102-0801 (Print)
Volume 1. Issue 1

LTU-JACE 2026 VOL.1 (1):

Drone and Electrical Resistivity Tomography (ERT) survey assisted slope instability risk assessment: A case study of Phyllitic landslide in Lesser Himalayas of Nepal

Buddhi Raj Joshi[1*], Netra Prakash Bhandary[2], Indra Prasad Acharya[3], Niraj KC[4]

[1] School of Engineering, Faculty of Science and Technology, Pokhara University, Kaski

[2] Faculty of Collaborative Regional Innovation, Ehime University, Matsuyama, Japan

[3] Department of Civil Engineering, Pulchowk Campus, Institute of Engineering, TU, Nepal

[4] Institute of Engineering and Information Technology, Lumbini Technological University, Banke, Nepal

*Corresponding Email: buddhi.rajjoshi@pu.edu.np

Received: 7 December 2025 / Accepted: 1 February 2026 / Published: 1 March 2026

Abstract

This study investigates the geological and geotechnical drivers of roadside slope failures along the Khanigaon Rural Municipality-2 (Likhu) road section in Nuwakot, Nepal, where excavation for road expansion has triggered landslides with significant socio-economic consequences. Geologically situated within the Seti Formation, the area consists of grey-greenish gritty phyllites and conglomerates, which were analyzed through a combination of Electrical Resistivity Tomography (ERT) and laboratory testing. The investigation identified a critical slip surface between 1 m and 6 m depth within Sandy Silt (ML) and Sandy Lean Clay (CL) soils characterized by low cohesion (1-11 kN/m^2*) and friction angles (*26.5-30°*). Stability modeling using the Limit Equilibrium Method (LEM) via Geo-studio and Slide2 software yielded an initial Factor of Safety (FoS)* (Geo-studio FoS=0.668, and Slide2 FoS=0.679) *as low as 0.668, confirming a high risk of soil slope failure despite rock stability. While the removal of loose materials was found insufficient to stabilize the site* (Geo-studio FoS=0.828, and Slide2 FoS=0.832*), a proposed integrated design comprising a reinforced concrete shear wall, concrete cribs, and 25 mm diameter anchor bolts successfully increased the FoS to 1.84. This research concludes that combining these structural reinforcements with bio-engineering vegetation offers a sustainable and technically sound solution for Himalayan infrastructure restoration.*

Keywords: *Geotechnical, Geophysical, Landslide, Roadside slope failure, Factor of safety.*

1. Introduction

Landslide is the downslope movement of soil, rock, and debris under the influence of gravity(Arisanty et al., 2022; Kolapo et al., 2022). Landslides can result in significant harm to social and economic infrastructure, and environmental elements. The occurrence of frequent catastrophic mass movements in the Himalaya that cause the loss of infrastructure and human lives, pose a threat to millions of people (Dubey et al., 2023; Sati & Kumar, 2022). Nepal Himalayas is a product of collision between Indian and Eurasian plates. The coupling effect of seismo-tectonic movement and Asian rainfall is generating numerous landslides in the Nepal Himalayas. The fragile geology, rugged topography and steep slope are favourable conditions for slope stability. Previous researchers (Dangi, et al., 2019; Sati & Kumar, 2022) entioned that the generation of landslide is mainly due to non-engineering road construction practices in Nepal. It is evident that the occurrences of landslide are widespread near the road. Tiwari and Hideaki (1998) have mentioned that Nepal should change its conventional landslide prevention practices to the appropriate one as landslides are increasing in recent years. The causes of landslides are interaction of intense rainfall, seismicity, change in water level, storm waves or rapid stream erosion, geology, land cover, slope geometry, groundwater saturation, slope cut, vegetation cover, and anthropogenic activities are the major factors for the landslide generation (Gariano & Guzzetti, 2016). The landslide occurs with the interactions of one or more triggering factors where one hazard triggers another or increases the probability of others occurring (Gill & Malamud, 2014). Rainfall and roadside slope cut-induced landslides are common and frequent triggering factors for landslides in the mountainous region. The previous study based on 55-years of landslides and rainfall record in the Himalaya suggested that many landslides in occurred under the influence of 5 hours to 90 days of rainfall durations (DAHAL, 2012).

The United Nations has emphasized disaster and climate risk reduction as a core component of sustainable development, integrating these priorities across all levels of planning through the Sustainable Development Goals (SDGs). Among natural hazards, landslides pose a serious threat to linear infrastructure, particularly road networks in mountainous and developing regions, where they frequently cause loss of life, disruption of mobility, and significant economic damage. The International Disaster Database (EM-DAT) reports that landslides account for approximately 4.9% of all natural disaster events and 1.3% of total fatalities between 1990 and 2015, with Asia experiencing nearly 54% of global landslide events (Guha-Sapir & Checchi, 2018). Roads are especially vulnerable due to slope cutting, inadequate drainage, and increasing exposure to intense rainfall and seismic activity. Globally, 55,997 fatalities

were recorded from 4,862 landslide events between 2004 and 2016, many of which were associated with transportation corridors (Froude & Petley, 2018). In Nepal, the 25 April 2015 Gorkha earthquake triggered over 21,000 landslides, severely damaging strategic road links and isolating communities (Valagussa et al., 2021). Furthermore, regional landslide inventories developed using remote sensing techniques in Nepal's Far-Western Region identified 26,350 landslide events, highlighting the high susceptibility of road-adjacent slopes over extended periods (Muñoz-Torrero Manchado et al., 2021). These findings underline the critical need for systematic assessment, monitoring, and mitigation of landslide hazards along road sections to enhance infrastructure resilience and ensure sustainable transportation development.

Nepal is a predominantly mountainous country with high tourism potential and an increasing demand for rapid transportation infrastructure development. However, unplanned and accelerated road construction activities have significantly contributed to slope instability, posing serious challenges to the sustainability of road networks. In particular, irrational hillslope excavation during road construction has increased the susceptibility of slopes to shallow rainfall-induced landslides. Non-engineered road construction practices—characterized by informal excavation methods without proper planning, design, drainage, or slope protection—have substantially amplified landslide risks across Nepal (Pradhan et al., 2022).

Rainfall-induced landslides along road cut slopes are further influenced by continuous excavation and modification of natural slopes. The reactivation of ancient landslides often manifests as retrogressive movement caused by prolonged engineering excavation, which results in rock mass unloading and degradation of the mechanical properties of the soil–rock mixture (He et al., 2019). From a geotechnical perspective, rainfall infiltration reduces soil shear strength through increased hydrostatic pressure, dynamic loading, and the loss of matric suction (Kim et al., 2015). Previous studies have demonstrated that prolonged or intense rainfall increases the degree of saturation in near-surface soils, leading to a reduction in suction and shear strength and ultimately triggering slope failure (Islam et al., 2021).

In the present study area, the landslide was triggered by the combined effects of irrational road construction practices and intense rainfall. Although an immediate remedial measure in the form of a gabion wall was implemented, it failed to adequately support the backfill material, resulting in outward bulging and continued instability. This failure highlights a critical limitation in current slope management practices. Existing guidelines issued by the Government of Nepal for rural road slope excavation lack site-specific geological and geotechnical characterization, limiting their effectiveness in landslide risk mitigation (Paudyal et al., 2023). Accurate estimation of slip surface depth and overburden thickness is therefore essential for reliable slope stability assessment and effective design of stabilization measures.

Reliable subsurface characterization can be achieved through the integration of geophysical and geotechnical investigations, such as electrical resistivity tomography (ERT) combined with laboratory testing, which together provide comprehensive information on geological structures and material properties (Dezert et al., 2019). Similar integrated approaches have successfully enhanced the understanding of landslide mechanisms in complex terrains, such as in Chira town, Ethiopia (Pasierb et al., 2019). However, many studies have not sufficiently examined the relationship between soil types and landslide occurrence, nor have they adequately evaluated the effectiveness of various remediation measures.

For sustainable infrastructure development, it is essential to incorporate geological, geotechnical, and site-specific parameters into slope stabilization and ecological restoration design. Although geotechnical investigation–based preventive measures have been proposed for debris landslides along unstable road cut slopes in the Himalayan region of India (Prakasam et al., 2020), detailed evaluation of subsurface conditions and material properties is often lacking. Field-based evidence suggests that road cut slopes excavated during the dry season remain temporarily stable due to soil suction, but infiltration of monsoon rainfall leads to saturation at shallow depths, resulting in suction loss and reduced soil strength, ultimately causing slope failure (Meena & Piralilou, 2019).

In this study, slip surface identification using electrical resistivity tomography (ERT), laboratory-based evaluation of soil properties for bearing capacity assessment, detailed geological mapping, and high-resolution topographic surveying were carried out. Slope stability was analyzed by estimating the Factor of Safety (FoS) using the Limit Equilibrium Method (LEM) based on the Mohr–Coulomb failure criterion (Ismail et al., 2021). The analyses were performed using GeoStudio (SLOPE/W) and Slide2 software, incorporating geotechnical parameters obtained from laboratory tests and topographic data derived from a high-resolution Digital Terrain Model (~30 cm).

In addition to structural stability, ecological restoration of roadside slopes must be scientifically evaluated to ensure long-term sustainability. Although bioengineering techniques are widely recognized for erosion control, slope stabilization, and ecological restoration (Raut & Gudmestad, 2017), restoration effectiveness varies spatially and temporally (Wang et al., 2021). Incorporating indigenous knowledge and locally adapted vegetation can help preserve site originality and accelerate restoration outcomes. Despite their potential, integrated geophysical–geotechnical approaches combined with ecological restoration strategies remain underutilized in the Nepalese context.

Therefore, this study aims to investigate the complex interaction between rainfall and road cut slope instability in the Nepal Himalaya by analyzing a representative

landslide case from central Nepal. The study integrates drone-based topographic surveying, electrical resistivity tomography, geotechnical investigation, numerical slope stability analysis, and bioengineering-based restoration measures to propose sustainable solutions for roadside slope stabilization

1.1 Study Area

The landslide is located along the road section of Likhu Rural Municipality Ward Number-2 of Nuwakot District of Nepal (Latitude: 27°56'03.61" N, and Longitude: 85°11'51.33" E , and elevation of 1027 m from a.s.l.) (Fig.1). In geological terms, the landslide has 160 - 180° (SE-S) failure orientation plane with failed slope angle of head to crown is ~ 34°. Before 2021 AD the slope remained relatively stable over time though the road section was constructed during 1995 AD. The problem was encountered due to rainfall and toe cutting during road extension, resulted in the roadside slope failure in the year of 2021 AD. Furthermore, the gabion structure was constructed in 2022 AD, further excavation during the trenching of the foundation lead to the failure of the soil mass in the form of landslide.The landslide is in irregular shape length of about 65 m and breadth is about 80 m which covers the area of about 5000 m^2.

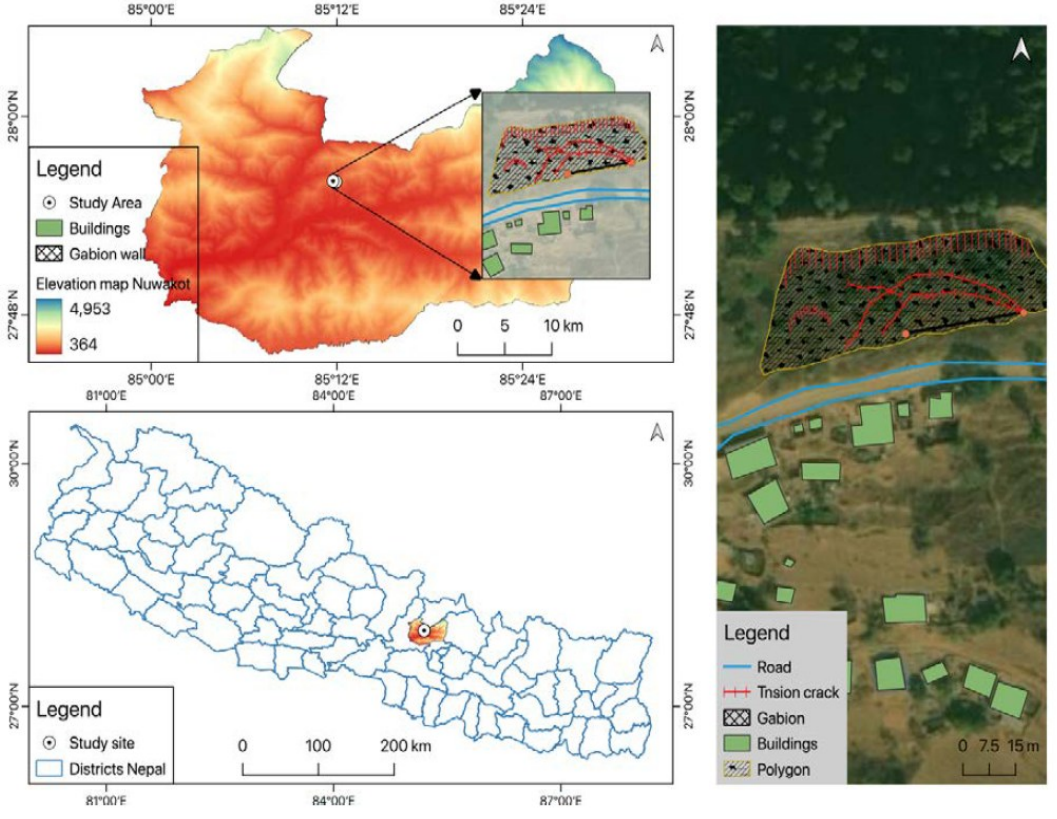

Figure 1: Locational Map of the study area.

1.2 History of the landslide:

Nuwakot district also suffered from the earthquake triggered landslide and earthquake-induced hazard map has been prepared though the proposed site was not vulnerable during that period (Dangi et al., 2019; Joshi et al., 2017). The aerial photographs of the area from 2021 AD suggest that the area is relatively stable and landslide events are recent. The image shown in Figure 1 indicates that there is an existing road section that was constructed around 1995 AD and had remained relatively stable over time. The problem was encountered during the road extension which involves the toe cutting of previously steadied slope, resulted in the roadside slope failure in the year of 2021 AD. Furthermore, the gabion structure was constructed in 2022 AD, further excavation during the trenching of the foundation lead to failure of the soil mass in the form of landslide.

Figure 1: Figure shows the aerial photograph of the study area

2. Methodology

2.1. Geology of the study area:

The study area lies within the Upper Pre-Carabean to late Paleozoic era, especially in the Seti formation (English et al., 2000). The lithology of the area consists of Grey greenish grey gritty phyllites gritstones with conglomerates with partly intruded

massive white quartzite in upper part. The following figure highlights the regional geology of the area (Figure 3).

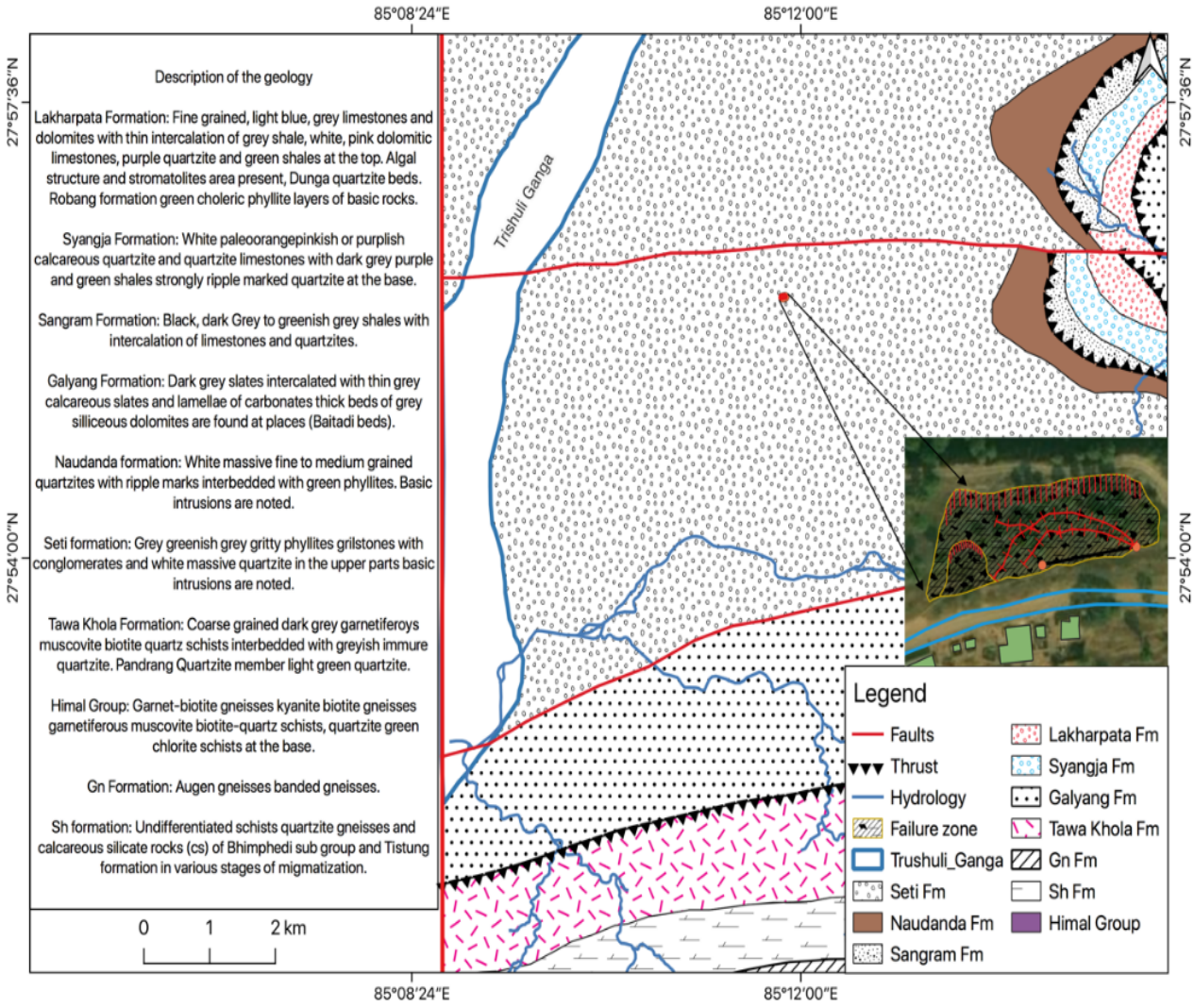

Figure 3: The geological map of the study area (inventory on the zoom)

2.2 Ortho-photo interpretation:

The unmanned aerial vehicle (UAV) is utilized for the monitoring of the landslide and produce high-resolution digital elevation models (DEM), orthophotos, and aerial photos based density point clouds obtained from structure-from-motion (Eker et al., 2018; Tian et al., 2020).The UAV captured images that were processed in Pix4Dmapper and obtained Ortho-photo and Digital Terrain Model (DTM) having a resolution of 0.3 meters (30 cm). The houses observed in the Ortho-photo were digitized and the linear features such as the drainage and debris flow channel were delineated. The contour of the terrain was prepared from the DTM accordingly the cross-sectional profile of the terrain was constructed, and road alignment was overlaid.

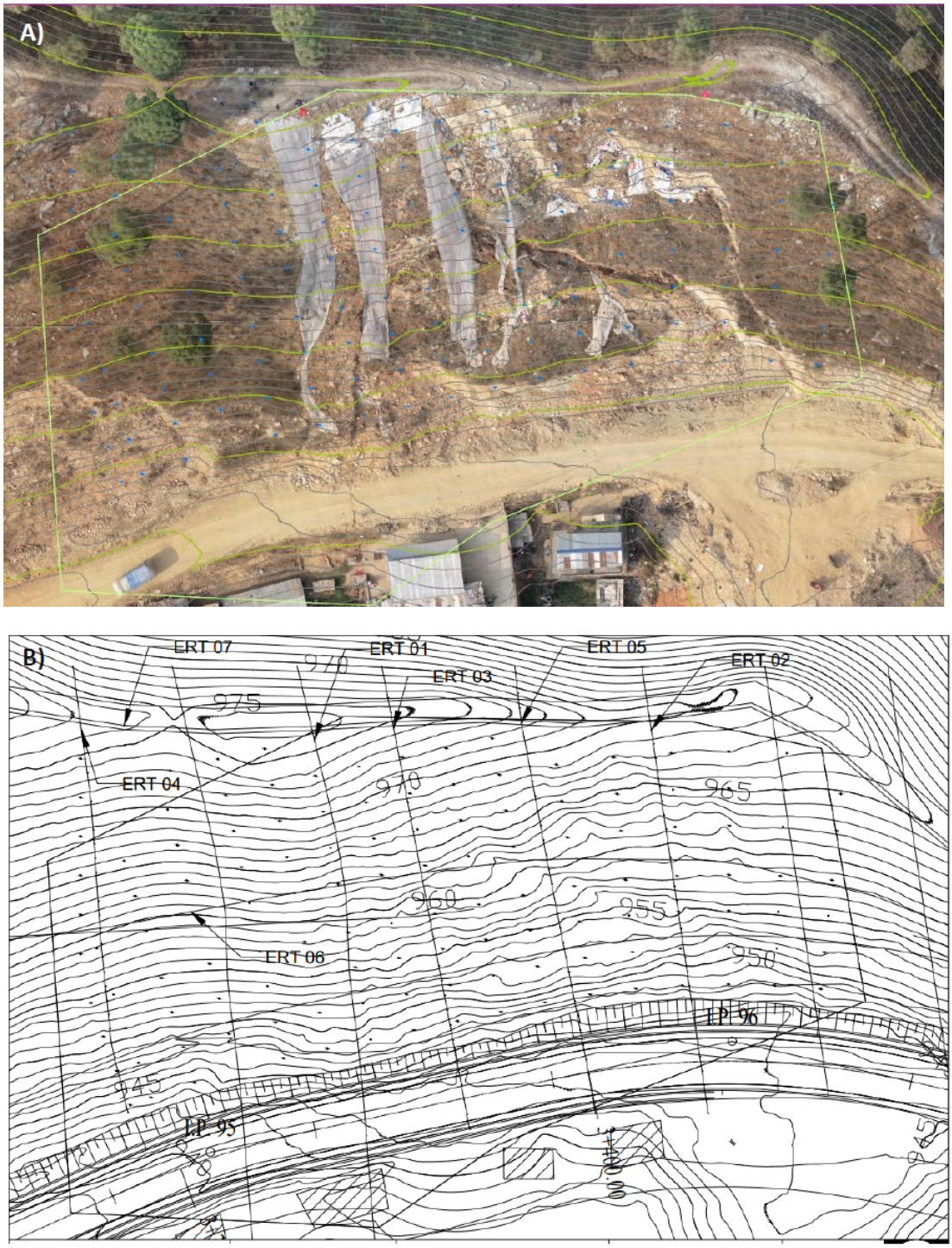

Figure 4: A) Orthophoto of landslide and B) contour map aligned with the designed road.

2.3 Electrical Resistivity Tomography (ERT):

The geophysical survey based on ERT is useful to identify the slip surface and groundwater table which can be utilized for the stability analysis (Haider et al., 2023;

Sigdel & Adhikari, 2020). The ERT survey was conducted with WDJD-4 Resistivity/IP equipment. The District Map, GPS, Drone, Photographic Camera, Brunton Compass, and Geological Hammer were used during the data collection. Due to the undulated site conditions, topographic correction has been adopted for the ERT profiling. Field data were gathered to obtain a continuous coverage of the sub-surface along the line of investigation which illustrates different resistivity zones due to presence of different lithological types (Figure 5).

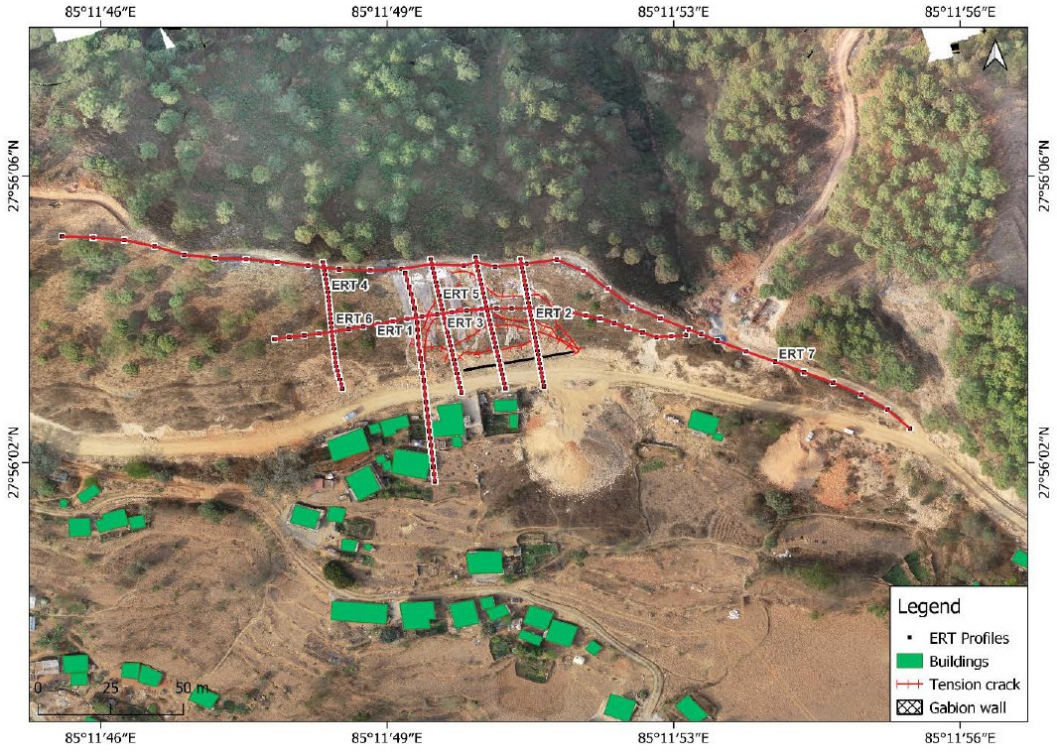

Figure 5: ERT profiles conducted in the study area.

The detail of the ERT profile that has been taken for the analysis has been presented which illustrates the general background of the ERT survey (Table 1)

Table 1: Table shows background of ERT Survey

ERT profile	Length of ERT (m)	Thickness of Moved mass (m)
1	87	2-6
2	58	1-5
3	58	1.5-5
4	58	1.5-4
5	58	2.5-6

3. Result and Discussion

Field investigation and orthophoto interpretation revealed the presence of tension cracks and distinct lines of movement across the slope. The terrain slope varies between 32° and 42°, with a maximum elevation difference of approximately 37 m. The road is located on the south-facing ridge of the hill, where the slope has become unstable due to the absence of persistent groundwater conditions, whereas the north-facing slope remains relatively stable, as shown in Figure 4.

3.1 Interpretation of ERT profile

The very low resistivity zone <1200 Ohm-m which represents silt with sand and less gravel. The low resistivity zone 1200 to 2400 Ohm-m which represents weak rock mass or sheared rock. The moderate resistivity zone 2400 to 9600 Ohm-m represents unsaturated weathered rock. The high resistivity zone 2400 to 38400 Ohm-m denotes the moved mass (unsaturated silt-fine sand with gravels and gravels with silt-sand), and very high resistivity zone >38400 Ohm-m denotes unsaturated hard to fractured rock. The similar results were presented in the previous research conducted in Ngozumpa glacier of Nepal (Thompson et al., 2017). The detail sub-surface condition and slip surface estimation has been presented below (Figure 6).

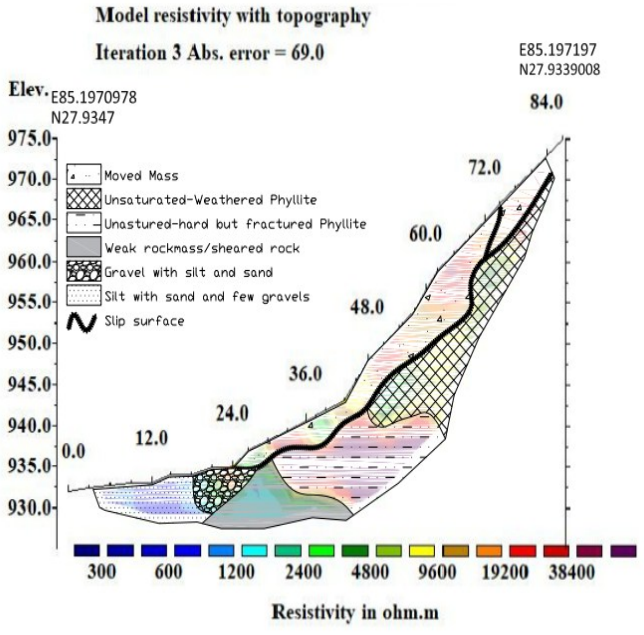

(a)

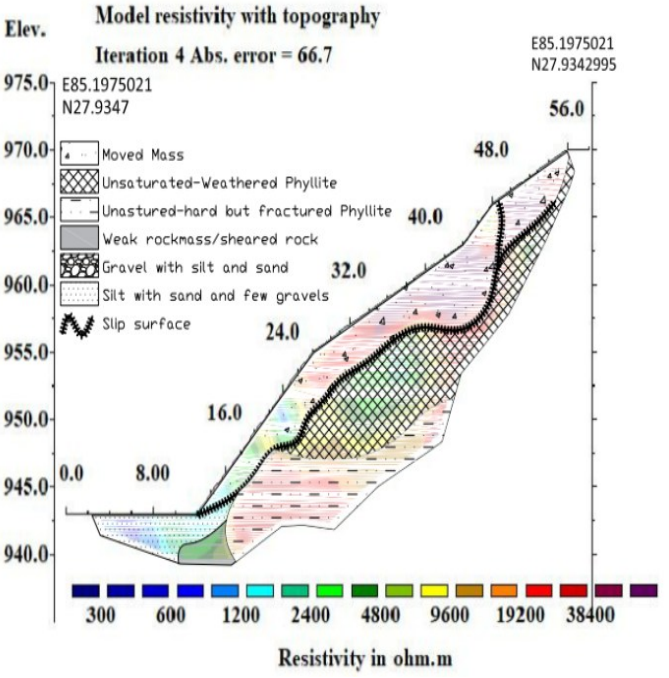

(b)

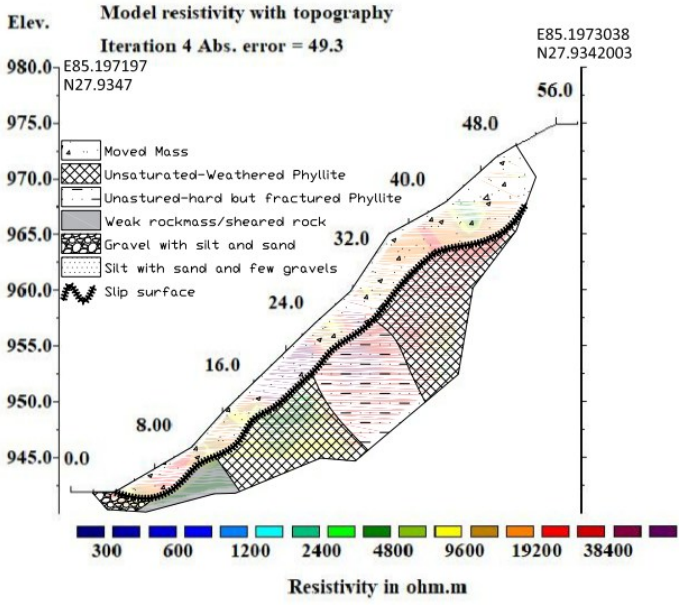

(c)

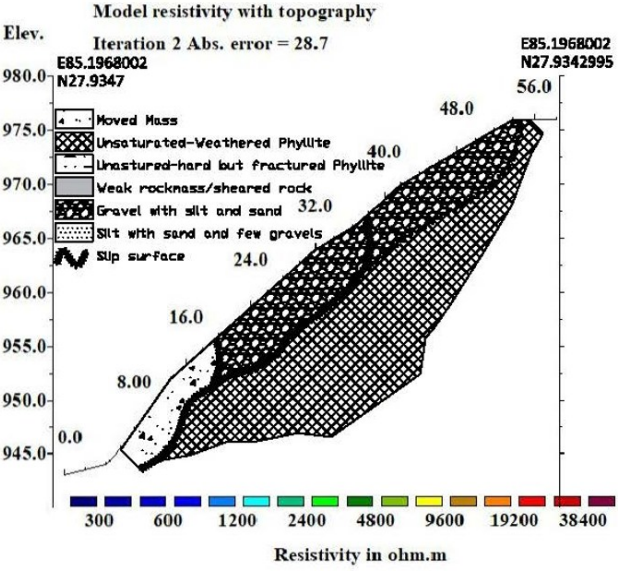

(d)

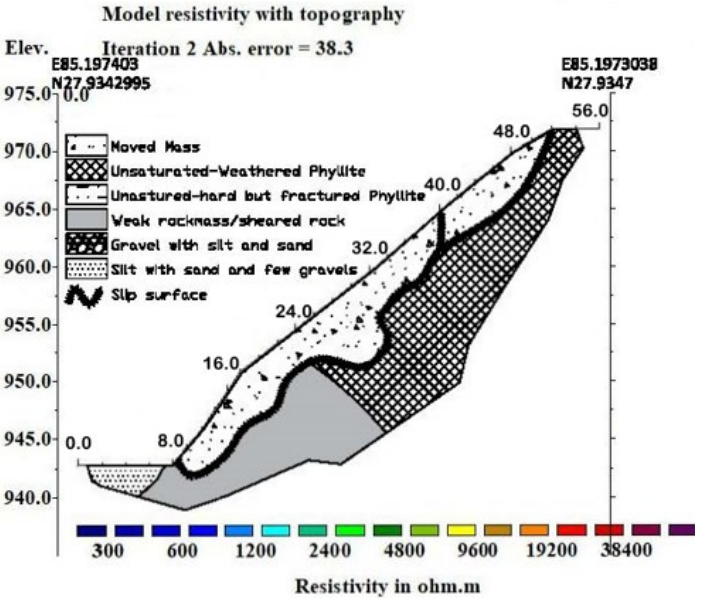

(e)

Figure 6: a) ERT profile 1 b) ERT profile 2 c) ERT profile 3 d) ERT profile 4, and e) ERT profile 5 of the study area with slip depth interpretation.

3.2 Geotechnical Investigation:

The soil lithology of the area is dominated by fine grained silty and clay minerals and rock lithology is dominated by the metamorphic rock Phyllites. Slope stability analysis was performed to determine the failure mechanism of soil and create a stable slope at the proposed site. The existing slope characterization and strength properties of the

soil were determined from fieldwork and laboratory analysis. Geotechnical properties of the soil samples collected from the following locations have been derived from the laboratory testing (Figure 7).

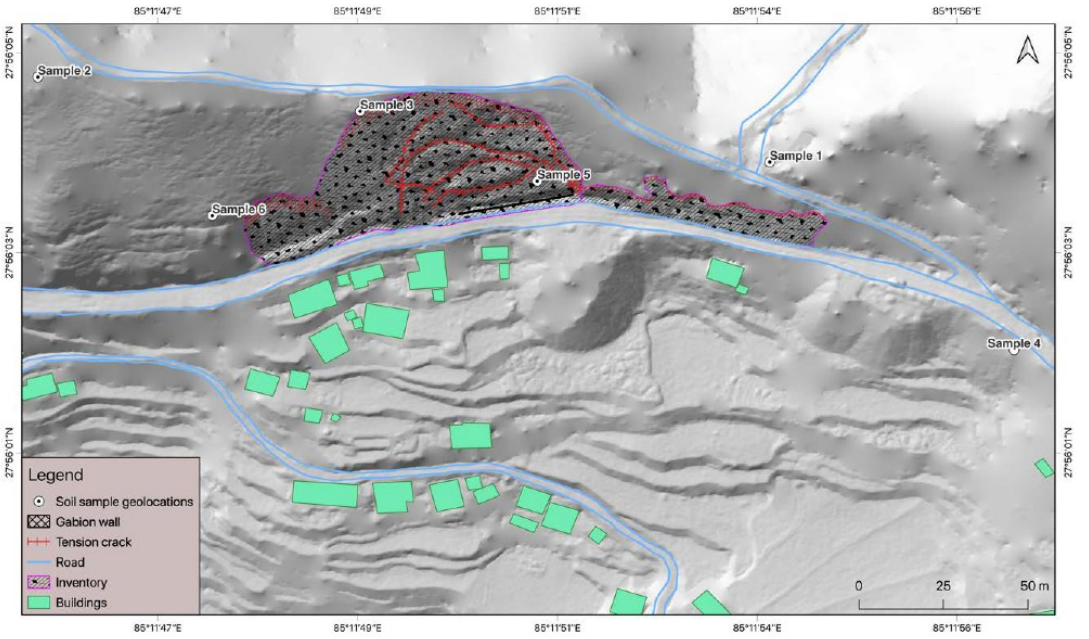

Figure 7: Inventory map (with hill-shade overlay) shows the location of soil samples collected.

The following laboratory tests have been carried out to assess the physical properties of the soil which are critically analysed for the stability analysis and design.

Table 2: Type and number of laboratory tests performed in this study.

Test	Test frequency	Standard	Significance of the study
Sieve analysis	6	IS: 2386 (Part 1)-1963	Particle size distribution of coarse-grained soil having particle size of<4.75->0.075mm
Hydrometer	6	IS: 2720 (Part 4)	Particle size distribution of fine-grained soil having particle size of<0.075mm
Natural Moisture Content	6	IS: 2720 (Part 2)	Moisture content in the soil at natural condition

Atterberg Limits	6	IS: 2720 (Part 5)	Evaluate the critical water contents of fine-grained soils before changing its state.
Specific gravity	6	IS: 2720 (Part 3)	Evaluation of porous behavior of soil for the estimation of phase relationship and FoS
Direct Shear	6	IS: 2720 (Part 15)-1986	To find Cohesion (c), Angle of Internal Friction (Ø) and Density of soil (γ) that are used for FoS calculation
Hydraulic Conductivity	1		

3.2.1 Index properties of soil:

According to the Unified Soil Classification System (USCS), the soil is Sandy silt with and without gravel of ML and Sandy Lean Clay with Gravel or sand of CL group that contains 5-26% clay (Table 3 and Table 4). The liquid limit of soil samples resembles value ranges from 38-47% which indicates soil sample 2, and 5 losses its shear strength and becomes liquid-like at a lower water content than soil samples S1, S3, S4 and S6 (Table 3). The plastic limit of the soil ranges from 20-27% except soil sample 5 which indicates that there is no clay content (Table 3).

Table 3: Index properties of soil samples.

Soil Sample	**% passing 0.075mm**	**% passing 0.005mm**	**D_{60}**	**D_{30}**	**D_{10}**	**C_u**	**Atterberg Limit (%)**			**USCS* Soil Classification**	
							LL	**PL**	**PI**	**Group**	**Description**
1	62.14	32.000	0.052	-	-		43	27	16	ML	Gravelly Silt
2	78.59	34.38	0.022	-	-		40	26	14	ML	Silt with Sand
3	50.15	21.50	0.080	-	-		45	26	19	ML	Sandy Silt with Gravel
4	44.78	17.00	1.25	0.0015	0.077		42	20	22	CL	Sandy Lean Clay with Gravel

5	30.52	7.00	2.00	0.006	0.025	38	NP	NP	ML	Sandy Silt with Gravel
6	53.11	15.00	0.60	0.005	3.33	47	27	20	CL	Gravelly Lean Clay with Sand

Notations: LL=Liquid Limit, PL=Plastic Limit, and PI=Plasticity Index

Table 4: Index properties of soil samples.

Soil Sample	**Sieve Analysis (%)**			
	Gravel	**Sand**	**Silt**	**Clay**
1	23.31	14.55	40.14	22.00
2	4.61	16.80	52.59	26.00
3	19.71	30.15	32.15	18.00
4	25.38	29.84	32.78	12.00
5	31.93	37.55	25.52	5.00
6	25.29	21.60	38.11	15.00

Grain size and their nomenclature: 50mm - 4.75mm is considered as Gravel, 4.75mm - 0.075mm is considered as Sand, 0.075mm - 0.002mm is considered as Silt, and < 0.002mm is considered as Clay.

3.2.2 Specific gravity:

The specific gravity of the soil ranges from 2.592 to 2.827 which indicates that the Sandy Clay has minimum value and Sandy Silt with Gravel has maximum value (Table 5).

Table 5: Specific gravity of soil

Soil Sample	Specific gravity of Soil Sample
1	2.719

2	2.712
3	2.690
4	2.708
5	2.827
6	2.592

3.2.3 Strength parameters:

Direct Shear test was carried out on 6 umber of soil sample samples retrieved from different locations. The graph between normal and shear stress has been plotted (Figure 8). The friction angle value indicates that the friction angle of sandy soil decreases with increase in confining pressure, thus implying a circular soil failure envelope. The typical sandy soil has negligible shear strength at zero confining stress which can generally be modelled with a cohesion value of zero (Sigdel & Adhikari, 2020).

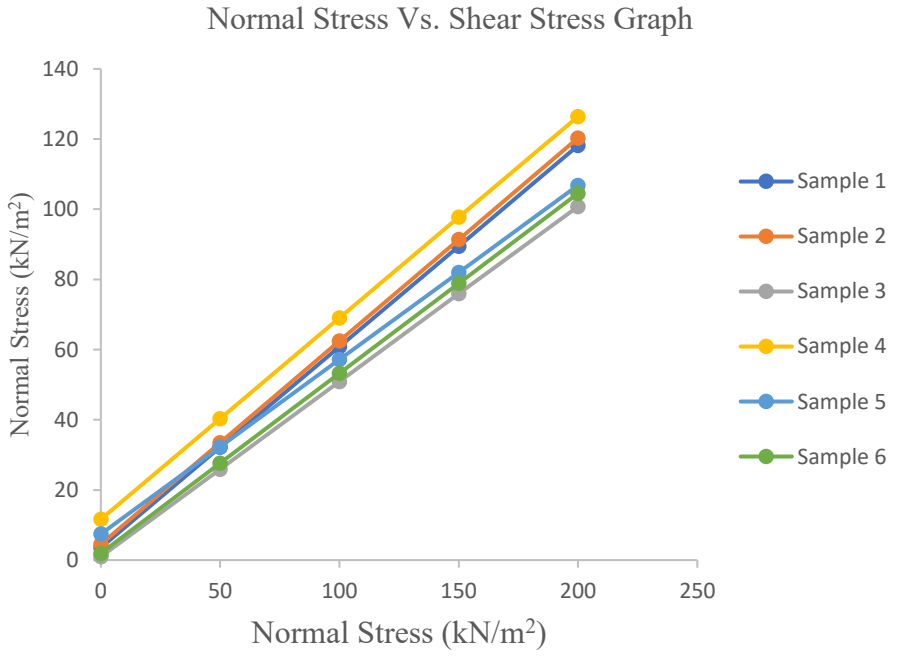

Figure 8: Normal stress vs. Shear stress curve for 6 different locations.

The cohesion (c) and angle of internal friction (ϕ^o) of the soil was found in the range of 1.0 to 11.60 kN/m^2 and 26.5^o to 30^o respectively which can be tabulated in the following table 6.

Table 6: Geotechnical parameters of soil samples.

Soil Sample	Natural Moisture Content (NMC %)	γ_{dry} (kN/m^3)	γ_{bulk} (kN/m^3)	Direct Shear	
				c (kN/m^2)	ϕ °
1	27.32	12.28	15.635	3.6	30.0
2	24.13	12.13	15.057	4.5	30.0
3	29.97	14.25	18.521	1.0	26.5
4	24.21	15.23	18.917	11.6	30.0
5	17.78	15.49	18.244	7.4	26.5
6	24.01	13.02	16.146	2.0	27.0

Natural moisture content of the soil varies from a minimum value of 17.78% to a maximum value of 29.97%. Bulk unit weight determination on selected samples of soil shows the values in the range of 15.057kN/m3 to 18.917kN/m3 and that of dry density value ranges from 12.12kN/m3 to 15.49 kN/m3. Unit weight, cohesion, and friction angle parameters are considered for the factor of safety analysis.

3.3 Slope Stability analysis:

Slope stability analysis is the core aspect of the research so that slope failure can be handled to ensure the safety of the infrastructure as well as the people living in the vicinity. The stability analysis has been done by adopting two approaches which includes a) rock slope stability analysis, and b) soil slope stability analysis.

3.3.1 Rock slope stability analysis:

The DIPs software has been adopted to estimate the rock slope stability which employs the graphical approach for the analysis. It analyses the stability of the slopes with complex geometries that include multiple dip direction and variable dip angles. The software also incorporates different methods, including limit equilibrium and kinematic analysis, to determine the factors influencing slope stability (Rahman et al., 2023). Limit equilibrium analysis assumes the equilibrium between the driving and resisting forces acting on a slope. On the other hand, kinematic analysis is useful for identifying potential failure modes and their associated geometries. The analysis of 30 vectors for the Phyllite rock in the area shows that the area has low possibility of plane failures. The hill slope is placed concordant to the bedrock dip. However, the steeper terrain is not in the daylight for the failure, indicated that the slope failure is mainly

due to the toe excavation and the failure material is overlaying soil and detached rock blocks (Figure 9).

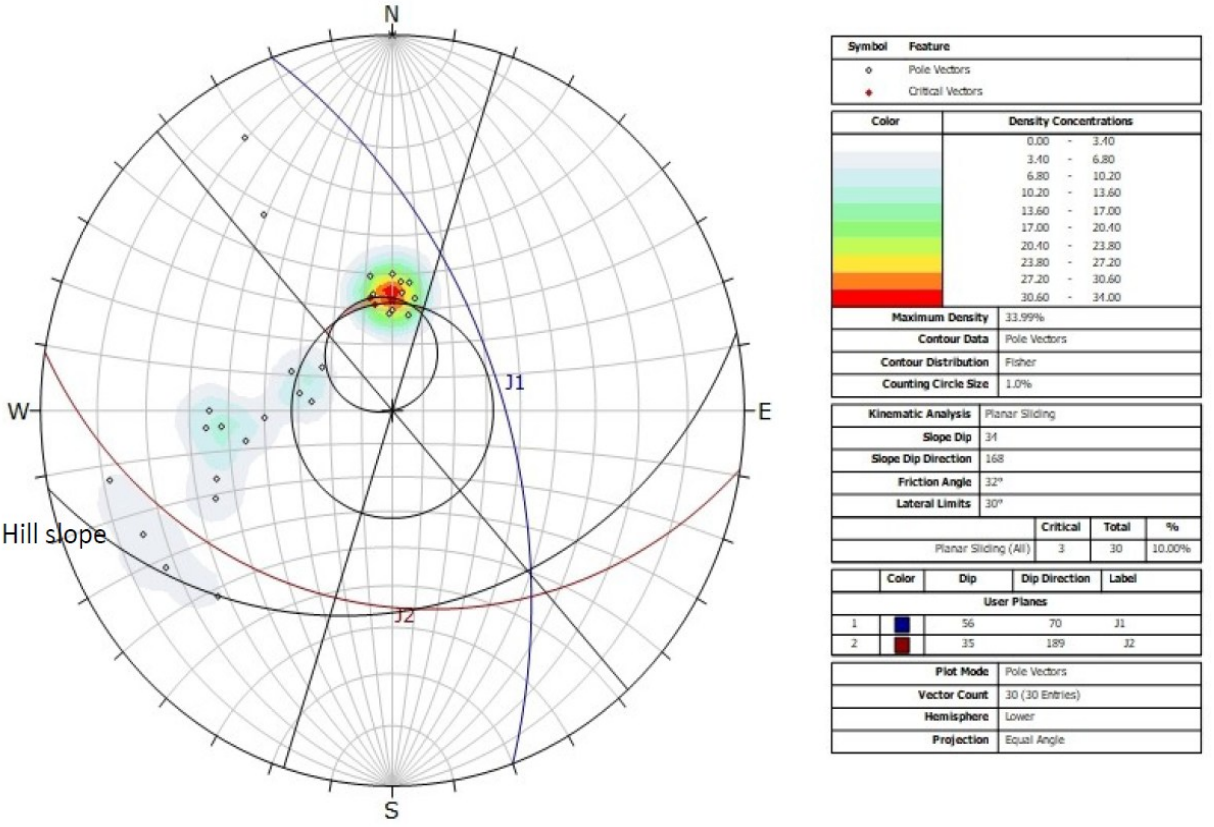

Figure 9: Rock slope stability analysis

3.3.2 Soil Slope stability:

The slope stability was assessed using the Geo-Studio Software (Package SLOPE/W) and Slice2 software that works on limit equilibrium model (LEM) for which laboratory analyzed geotechnical parameters obtained from the laboratory testing and topographical parameters obtained from high resolution Digital Terrain Model (~30 cm) were used. The Geo-studio and Slope2 software packages have been widely accepted software for the slope stability analysis using Bishops' method for the estimation of factor of safety (Geo-Studio, 2012; Salmasi et al., 2019; Su et al., 2022). The stability model was implemented for the soil profile (Figure 10, and Figure 11) depicted that the slope is unstable which has FoS less than 1 (Geo-studio FoS=0.668, and Slice FoS=0.679).

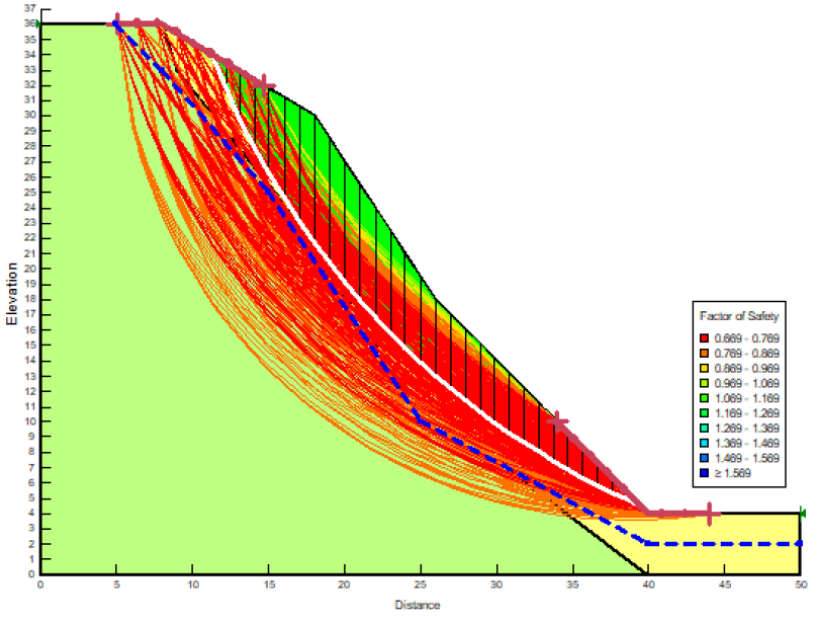

Figure 10: Limit Equilibrium Analysis (FoS) of the slope profile based on Geo-studio.

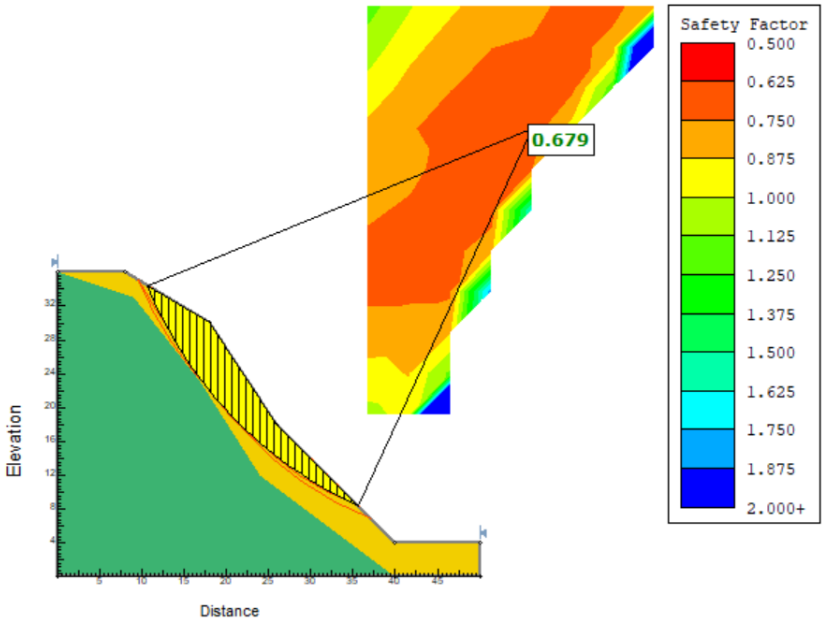

Figure 11: Limit Equilibrium Analysis (FoS) of the slope profile based on Slice2.

To achieve the roadside slope stable, firstly a model was constructed by removing the loose materials on the slope (i. e. removing the surcharge load) and checked the FoS with a 2-meters bench in the middle of the slope without anchor bolt. The model depicted FoS which is still lower than 1 indicates that the slope is still unstable (Geo-studio FoS=0.828, and Slide2 FoS=0.832).

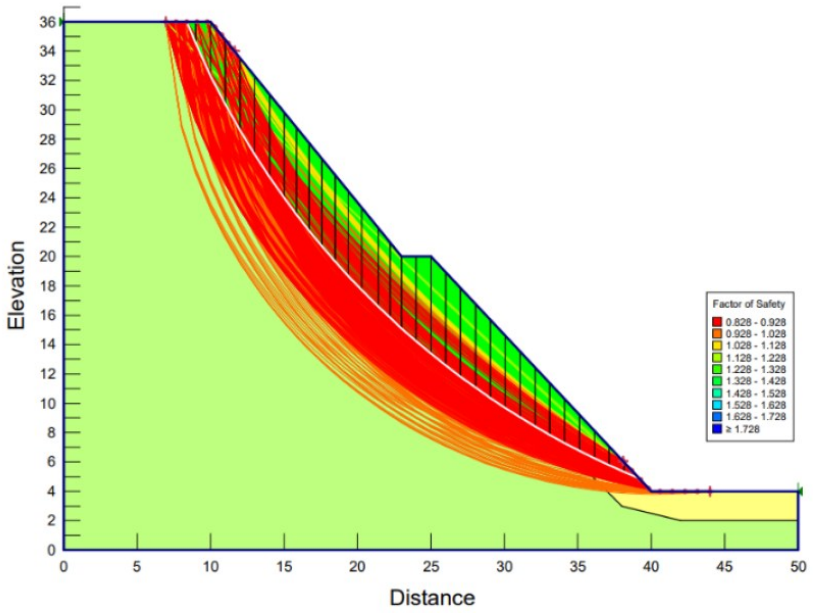

Figure 12: Limit Equilibrium Analysis (FoS) of the slope profile based on Geo-studio.

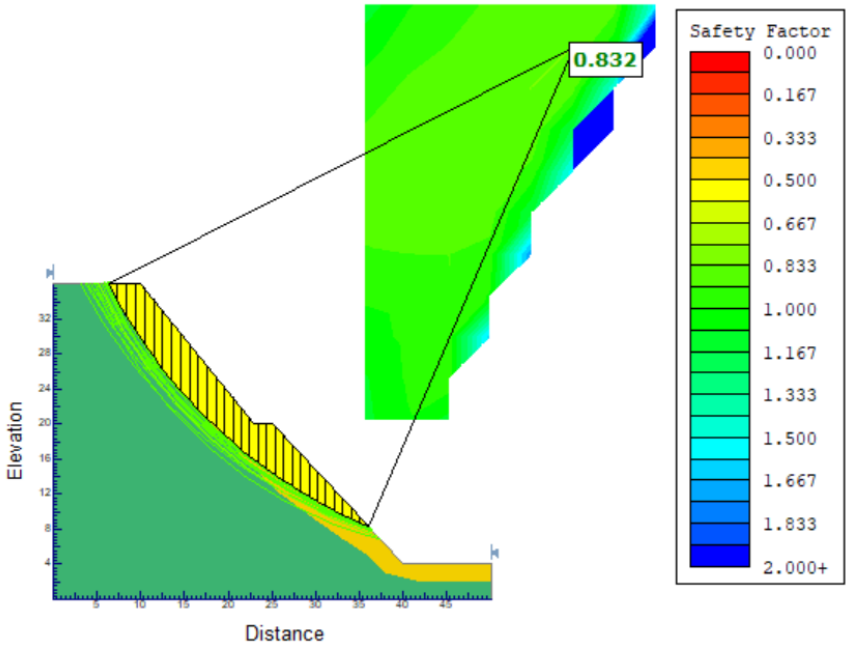

Figure 13: Limit Equilibrium Analysis (FoS) of the slope profile based on Slice2.

The above models clearly indicated the requirement of the Anchorage. Finally, a Geo-studio-based model was set for the reinforced concrete shear wall (Height=1.8 m, and Length=81 m), concrete crib (Size= 0.3m×0.3 m, and total length=1843m), and anchor bolts (Size= 25 mm diameter, bond length=3 m, and numbers=182) for 150kN/m^2 point load. The appropriate design-based stability analysis indicates that the slope became stable (FoS=1.84) (Figure 14).

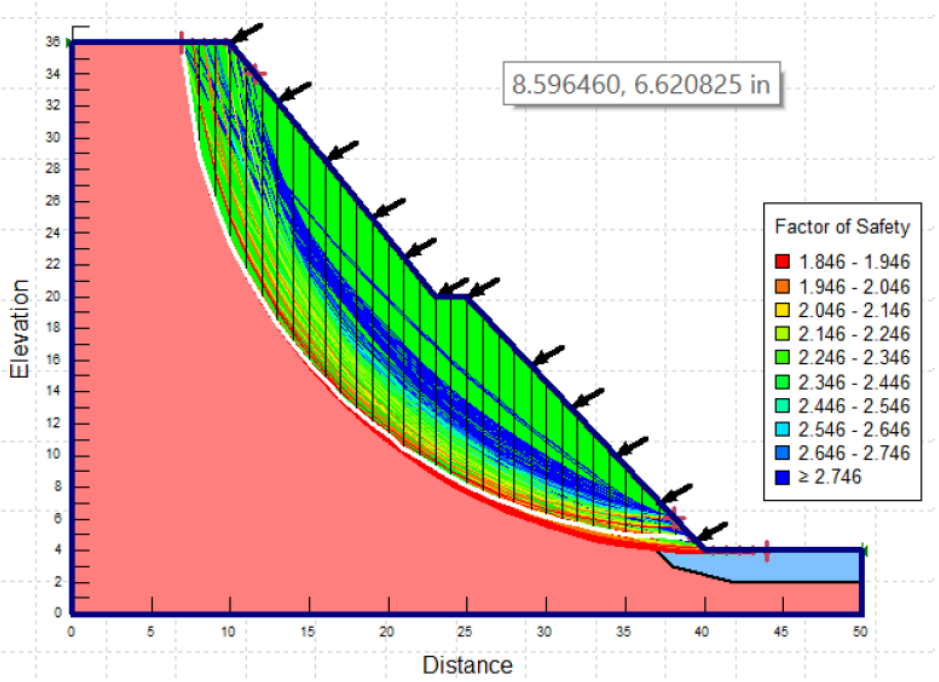

Figure 14: FoS Model with the point load of 150 kN/m^2.

4. Conclusions

The landslide induced by roadside slope cut along the road section of Khanigaon Rural Municipality-2, Likhu of Nuwakot district of Nepal is shallow and a non-uniform circular slip surface in nature. The field and laboratory investigations have been carried out to analyse the geological and geotechnical aspects of the landslides. Filed investigation reveals that there are no chances of rock slope failure, but the slope is unstable due to soil slope failure. The slope stability analysis of the existing condition reveals that the slope is not stable having the factor of safety (Geo-studio FoS=0.669, and Slide2 FoS=0.679). A model was constructed by removing the loose materials on the slope (i. e. removing the surcharge load) and checked the FoS with a 1.5-meters bench in the middle of the slope without anchor bolt depicted (Geo-studio FoS of 0.828, and Slide2 FoS=0.832), which is lower than 1 indicates that the slope is still unstable. The proposed Geo-studio-based model clearly indicates that there is the requirement of the anchorage system and construction of shear wall, concrete crib, and rock nail system has been proposed to make the slope stable. To withstand 150kN/m^2 point load 10-12 number of anchor bolts having length of 3m are required which suggest that the improved slope stability with FoS of 1.84. Based on the result analysis and the comprehensive design the following preventive measures are recommended for the slope stability.

a. Removal of loose earth material: It is suggested to remove the loose earth material from slope which results in the reduction of the surcharge load thereby increasing the FoS. The modelling also indicated that the removing of the loose earth material increases the FoS from 0.68 to 0.82.

b. Construction of RCC shear wall: Steel Reinforced Cement Concrete (RCC) shear wall is proposed along the hillside or the toe of the slope parallel to the roadside drainage. The share wall is 81-meter in length and 1.8-meter high along with the height of the foundation. A shallow shear wall has been proposed to reduce the cost and to support the concrete crib to be built on the hill slope.

c. Construction of concrete crib and anchors: The slope to be protected is long and the slope varies from 33-40 degrees below which settlement is located. Field Observation, modelling and design work depicted that the concrete crib along with the rock bolt is the best option in terms of cost, stability, and sustainability.

d. Vegetation: The restoration of the natural environment and ecology can be achieved by applying vegetation in the free space available between the cribs of the slope protection system.

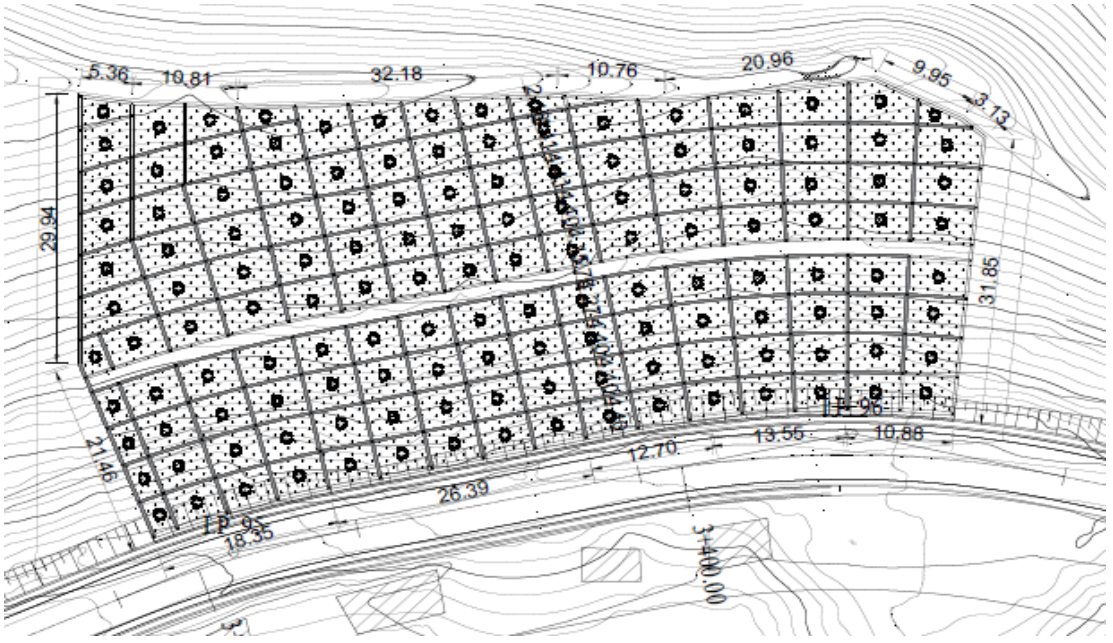

Figure 15: Plan for landslide structure

Data Availability Statement:

The data that support the findings of this study are available to the main author, upon reasonable request.

Acknowledgement:

This research was partly support by ‘‘Government of Bagmati Province, Ministry of Physical Infrastructure Development, Transport Infrastructure Directorate, Transport Infrastructure Development office, Nuwakot, Nepal. Mr. Birendra Kumar Bajracharya, Mr. Narayan KC, Mr. Bhuwan Awasthi, and Mr. Ujwal Maskey are sincerely acknowledged for their technical support during the preparation of this paper.

References

i. Arisanty, D., Hastuti, K. P., Saputra, A. N., Muhaimin, M., & Setiawan, F. A. (2022). Characteristic of mass movement in Riam Kanan watershed, Indonesia. *IOP Conference Series: Earth and Environmental Science*, *1089*(1). https://doi.org/10.1088/1755-1315/1089/1/012001

ii. DAHAL, R. K. (2012). Rainfall-induced Landslides in Nepal. *International Journal of Japan Erosion Control Engineering*, *5*(1), 1–8.

iii. Dangi, H., Bhattarai, T. N., & Thapa, P. B. (2019). An approach of preparing earthquake induced landslide hazard map: a case study of Nuwakot District, central Nepal. *Journal of Nepal Geological Society*, *58*, 153–162. https://doi.org/10.3126/jngs.v58i0.24600

iv. Dezert, T., Palma Lopes, S., Fargier, Y., & Côte, P. (2019). Combination of geophysical and geotechnical data using belief functions: Assessment with numerical and laboratory data. *Journal of Applied Geophysics*, *170*. https://doi.org/10.1016/j.jappgeo.2019.103824

v. Dubey, S., Sattar, A., Goyal, M. K., Allen, S., Frey, H., Haritashya, U. K., & Huggel, C. (2023). Mass Movement Hazard and Exposure in the Himalaya. *Earth’s Future*, *11*(9). https://doi.org/10.1029/2022EF003253

vi. Eker, R., Aydın, A., & Hübl, J. (2018). Unmanned aerial vehicle (UAV)-based monitoring of a landslide: Gallenzerkogel landslide (Ybbs-Lower Austria) case study. *Environmental Monitoring and Assessment*, *190*(1). https://doi.org/10.1007/s10661-017-6402-8

vii. English, N. B., Quade, J., Decelles, P. G., & Garzione, C. N. (2000). Geologic control of Sr and major element chemistry in Himalayan Rivers, Nepal. *Geochimica et Cosmochimica Acta*, *64*(15), 2549–2566.

viii. Froude, M. J., & Petley, D. N. (2018). Global fatal landslide occurrence from 2004 to 2016. *Natural Hazards and Earth System Sciences*, *18*(8), 2161–2181. https://doi.org/10.5194/nhess-18-2161-2018

ix. Gariano, S. L., & Guzzetti, F. (2016). Landslides in a changing climate. In *Earth-Science Reviews* (Vol. 162, pp. 227–252). Elsevier B.V. https://doi.org/10.1016/j.earscirev.2016.08.011

x. *Geo-Studio (2012) Version 7.1.0 User manual: Vol. 7.1.0 User manual*. (2012). Geo-Slope International.

xi. Gill, J. C., & Malamud, B. D. (2014). Reviewing and visualizing the interactions of natural hazards. In *Reviews of Geophysics* (Vol. 52, Issue 4, pp. 680–722). Blackwell Publishing Ltd. https://doi.org/10.1002/2013RG000445

xii. Guha-Sapir, D., & Checchi, F. (2018). Science and politics of disaster death tolls. In *BMJ (Online)* (Vol. 362). BMJ Publishing Group. https://doi.org/10.1136/bmj.k4005

xiii. Haider, S. A., Hussain, M., Ali, A., Abbasi, M. F., & Wani, S. (2023). Application of UAV photogrammetry and electrical resistivity tomography for characterization of a complex landslide: a case study from northwest Himalayas, Pakistan. *Natural Hazards*, *117*(3), 3043–3066. https://doi.org/10.1007/s11069-023-05977-0

xiv. He, K., Ma, G., Hu, X., Luo, G., Mei, X., Liu, B., & He, X. (2019). Characteristics and mechanisms of coupled road and rainfall-induced landslide in Sichuan China. *Geomatics, Natural Hazards and Risk*, *10*(1), 2313–2329. https://doi.org/10.1080/19475705.2019.1694230

xv. Islam, M. A., Islam, M. S., & Jeet, A. A. (2021). A geotechnical investigation of 2017 chattogram landslides. *Geosciences (Switzerland)*, *11*(8). https://doi.org/10.3390/geosciences11080337

xvi. Ismail, N. N., Ramli, A. B., & Mohd Pami, S. N. (2021). Comparison of factor of safety using different method of analysis for slope stability. *Journal of Applied Engineering Design and Simulation*, *1*(1), 52–58. https://doi.org/10.24191/jaeds.v1i1.28

xvii. Joshi, J., Bharadwaj, D., Paudyal, P., & Timalsina, N. (2017). Landslide inventory, susceptibility mapping and recommendation of the mitigation measures in Nuwakot District. *Journal of Nepal Geological Society*, *53*, 107–118. https://doi.org/10.3126/jngs.v53i0.23825

xviii. Kim, Y., Jeong, S., & Lee, K. (2015). Instability analysis of rainfall-induced landslides using hydro-mechanically coupled model. *15th Asian Regional Conference on Soil Mechanics and Geotechnical Engineering, ARC 2015: New Innovations and Sustainability*, 1002–1007. https://doi.org/10.3208/jgssp.KOR-07

xix. Kolapo, P., Oniyide, G. O., Said, K. O., Lawal, A. I., Onifade, M., & Munemo, P. (2022). An Overview of Slope Failure in Mining Operations. *Mining*, *2*(2), 350–384. https://doi.org/10.3390/mining2020019

xx. Meena, S. R., & Piralilou, S. T. (2019). Comparison of earthquake-triggered landslide inventories: A case study of the 2015 gorkha earthquake, Nepal. *Geosciences (Switzerland)*, *9*(10). https://doi.org/10.3390/geosciences9100437

xxi. Muñoz-Torrero Manchado, A., Allen, S., Ballesteros-Cánovas, J. A., Dhakal, A., Dhital, M. R., & Stoffel, M. (2021). Three decades of landslide activity in western Nepal: new insights into trends and climate drivers. *Landslides*, *18*(6), 2001–2015. https://doi.org/10.1007/s10346-021-01632-6

xxii. Pasierb, B., Grodecki, M., & Gwóźdź, R. (2019). Geophysical and geotechnical approach to a landslide stability assessment: a case study. *Acta Geophysica*, *67*(6), 1823–1834. https://doi.org/10.1007/s11600-019-00338-7

xxiii. Paudyal, P., Dahal, P., Bhandari, P., & Dahal, B. K. (2023). Sustainable rural infrastructure: guidelines for roadside slope excavation. *Geoenvironmental Disasters*, *10*(1). https://doi.org/10.1186/s40677-023-00240-x

xxiv. Pradhan, S., Toll, D. G., Rosser, N. J., & Brain, M. J. (2022). An investigation of the combined effect of rainfall and road cut on landsliding. *Engineering Geology*, *307*. https://doi.org/10.1016/j.enggeo.2022.106787

xxv. Prakasam, C., Aravinth, R., Nagarajan, B., & Kanwar, V. S. (2020). Site-specific geological and geotechnical investigation of a debris landslide along unstable road cut slopes in the Himalayan region, India. *Geomatics, Natural Hazards and Risk*, *11*(1), 1827–1848. https://doi.org/10.1080/19475705.2020.1813812

xxvi. Rahman, A. U., Zhang, G., A. AlQahtani, S., Janjuhah, H. T., Hussain, I., Rehman, H. U., & Shah, L. A. (2023). Geotechnical Assessment of Rock Slope Stability Using Kinematic and Limit Equilibrium Analysis for Safety Evaluation. *Water (Switzerland)*, *15*(10). https://doi.org/10.3390/w15101924

xxvii. Raut, R., & Gudmestad, O. T. (2017). Use of bioengineering techniques to prevent landslides in Nepal for hydropower development. *International Journal of Design and Nature and Ecodynamics*, *12*(4), 418–427. https://doi.org/10.2495/DNE-V12-N4-418-427

xxviii. Salmasi, F., Pradhan, B., & Nourani, B. (2019). Prediction of the sliding type and critical factor of safety in homogeneous finite slopes. *Applied Water Science*, *9*(7). https://doi.org/10.1007/s13201-019-1038-1

xxix. Sati, V. P., & Kumar, S. (2022). Environmental and economic impact of cloudburst-triggered debris flows and flash floods in Uttarakhand Himalaya: a case study. *Geoenvironmental Disasters*, *9*(1). https://doi.org/10.1186/s40677-022-00208-3

xxx. Sigdel, A., & Adhikari, R. K. (2020). Engineering Geological and Geotechnical studies of Taprang landslide, west-central Nepal: An approach for slope stability analysis. *Journal of Geological Research*, *2*(4). https://doi.org/10.30564/jgr.v2i4.2302

xxxi. Su, A., Feng, M., Dong, S., Zou, Z., & Wang, J. (2022). Improved Statically Solvable Slice Method for Slope Stability Analysis. *Journal of Earth Science*, *33*(5), 1190–1203. https://doi.org/10.1007/s12583-022-1631-3

xxxii. Thompson, S. S., Kulessa, B., Benn, D. I., & Mertes, J. R. (2017). Anatomy of terminal moraine segments and implied lake stability on Ngozumpa Glacier, Nepal, from electrical resistivity tomography (ERT). *Scientific Reports*, *7*. https://doi.org/10.1038/srep46766

xxxiii. Tian, Y., Owen, L. A., Xu, C., Ma, S., Li, K., Xu, X., Figueiredo, P. M., Kang, W., Guo, P., Wang, S., Liang, X., & Maharjan, S. B. (2020). Landslide development within 3 years after the 2015 Mw 7.8 Gorkha earthquake, Nepal. *Landslides*, *17*(5), 1251–1267. https://doi.org/10.1007/s10346-020-01366-x

xxxiv. Valagussa, A., Frattini, P., Valbuzzi, E., & Crosta, G. B. (2021). Role of landslides on the volume balance of the Nepal 2015 earthquake sequence. *Scientific Reports*, *11*(1). https://doi.org/10.1038/s41598-021-83037-y

xxxv. Wang, M., Liu, Q., & Pang, X. (2021). Evaluating ecological effects of roadside slope restoration techniques: A global meta-analysis. *Journal of Environmental Management*, *281*. https://doi.org/10.1016/j.jenvman.2020.111867

Competing Interests Disclaimer

Authors have declared that no competing interests exist. The data used for this research are commonly and predominantly used data in our area of research and country. There is absolutely no conflict of interest between the authors and other stakeholders because we do not intend to use these products as an avenue for any litigation but for the advancement of knowledge. Also, the research was not funded by any authorities rather it was funded by the personal efforts of the authors.